Endothelial ENPP2 (Ectonucleotide Pyrophosphatase/Phosphodiesterase 2) Increases Atherosclerosis in Female and Male Mice

Arteriosclerosis, Thrombosis, and Vascular Biology

BASIC SCIENCES

Endothelial ENPP2 (Ectonucleotide Pyrophosphatase/Phosphodiesterase 2) Increases Atherosclerosis in Female and Male Mice

Ela Karshovska,* Rokia Mohibullah,* Mengyu Zhu (朱梦瑜), Farima Zahedi, Dominique Thomas, Christiana Magkrioti, Claudia Geissler, Remco T.A. Megens, Mariaelvy Bianchini, Maliheh Nazari-Jahantigh, Nerea Ferreirós, Vassilis Aidinis, Andreas Schober

BACKGROUND: Maladapted endothelial cells (ECs) secrete ENPP2 (ectonucleotide pyrophosphatase/phosphodiesterase 2; autotaxin)—a lysophospholipase D that generates lysophosphatidic acids (LPAs). ENPP2 derived from the arterial wall promotes atherogenic monocyte adhesion induced by generating LPAs, such as arachidonoyl-LPA (LPA20:4), from oxidized lipoproteins. Here, we aimed to determine the role of endothelial ENPP2 in the production of LPAs and atherosclerosis.

METHODS: We quantified atherosclerosis in mice harboring loxP-flanked *Enpp2* alleles crossed with *Apoe*$^{-/-}$ mice expressing tamoxifen-inducible Cre recombinase under the control of the EC-specific bone marrow X kinase promoter after 12 weeks of high-fat diet feeding.

RESULTS: A tamoxifen-induced EC-specific *Enpp2* knockout decreased atherosclerosis, accumulation of lesional macrophages, monocyte adhesion, and expression of endothelial CXCL (C-X-C motif chemokine ligand) 1 in male and female *Apoe*$^{-/-}$ mice. In vitro, ENPP2 mediated the mildly oxidized LDL (low-density lipoprotein)-induced expression of CXCL1 in aortic ECs by generating LPA20:4, palmitoyl-LPA (LPA16:0), and oleoyl-LPA (LPA18:1). ENPP2 and its activity were detected on the endothelial surface by confocal imaging. The expression of endothelial *Enpp2* established a strong correlation between the plasma levels of LPA16:0, stearoyl-LPA (LPA18:0), and LPA18:1 and plaque size and a strong negative correlation between the LPA levels and ENPP2 activity in the plasma. Moreover, endothelial *Enpp2* knockout increased the weight of high-fat diet–fed male *Apoe*$^{-/-}$ mice.

CONCLUSIONS: We demonstrated that the expression of ENPP2 in ECs promotes atherosclerosis and endothelial inflammation in a sex-independent manner. This might be due to the generation of LPA20:4, LPA16:0, and LPA18:1 from mildly oxidized lipoproteins on the endothelial surface.

GRAPHIC ABSTRACT: A graphic abstract is available for this article.

Key Words: alleles ■ atherosclerosis ■ bone marrow ■ endothelial cells ■ lysophospholipids

Endothelial cells (ECs) play a critical role in the development of atherosclerosis. Disruption of laminar blood flow at predilection sites of atherosclerosis, such as branching points and curved aortic segments, is characterized by continuous, random changes in the shear stress direction, which makes the adaption of ECs to hemodynamic stress impossible.[1] The intrinsic inadaptability of ECs at predilection sites results in their apoptosis and inflammatory activation, which is compensated by a chronic repair process involving the regenerative proliferation of the endothelium. However, maladapted ECs are susceptible to additional injuries, such as hyperlipidemia, high glucose levels, and high blood pressure, promoting the formation of atherosclerotic plaques.[2]

Endothelial maladaptation is associated with the accumulation of lipoproteins, mainly LDLs (low-density

Correspondence to: Andreas Schober, Institute for Cardiovascular Prevention, Ludwig-Maximilians-University, Pettenkoferstraße 9b, 80336 Munich, Germany. Email aschober@med.lmu.de

*E. Karshovska and R. Mohibullah contributed equally.

Supplemental Material is available at https://www.ahajournals.org/doi/suppl/10.1161/ATVBAHA.122.317682.

For Sources of Funding and Disclosures, see page 1035.

Arterioscler Thromb Vasc Biol is available at www.ahajournals.org/journal/atvb

Nonstandard Abbreviations and Acronyms

CXCL	C-X-C motif chemokine ligand
EC	endothelial cell
ENPP2	ectonucleotide pyrophosphatase/phosphodiesterase 2
HFD	high-fat diet
LDL	low-density lipoprotein
LPA	lysophosphatidic acid
Lpar	lysophosphatidic acid receptor
LPC	lysophosphatidylcholine
Ly6G	lymphocyte antigen 6 complex locus G6
MAEC	murine aortic endothelial cell
moxLDL	mildly oxidized low-density lipoprotein
NF-κB	nuclear factor kappa light-chain enhancer of activated B cells
nLDL	native low-density lipoprotein
oxLDL	oxidized low-density lipoprotein
TNFα	tumor necrosis factor alpha

Highlights

- Endothelial ENPP2 (ectonucleotide pyrophosphatase/phosphodiesterase 2) expression promotes atherosclerosis in both sexes.
- Endothelial ENPP2 generates a strong correlation between LPA16:0, LPA18:0, and LPA18:1 plasma levels and plaque size.
- Mildly oxidized LDL (low-density lipoprotein) increases ENPP2-mediated LPA16:0, LPA18:1, and LPA20:4 production by endothelial cells.
- The local generation of lysophosphatidic acids on the surface of endothelial cells may contribute to the uncoupling of the ENPP2 activity from the lysophosphatidic acid levels in the circulation.

lipoproteins), in the intimal space, and vascular cells, including ECs, drive the oxidative modification of deposited LDL.[3–5] Mild oxidation of LDL generates various bioactive lipid compounds, such as lysophosphatidic acids (LPAs).[6–8] LPAs are phospholipids that contain a free phosphate group and a single fatty acyl chain in the glycerol backbone.[9,10] The predominantly 16-, 18-, and 20-carbon long fatty acids are either saturated, monounsaturated, or polyunsaturated.[10] LPAs act via the 6 G-protein–coupled LPA receptors, Lpar (lysophosphatidic acid receptor) 1 to 6, which have different binding affinities to the individual LPA species.[11] Unsaturated LPA20:4 increases atherosclerosis by upregulating CXCL (C-X-C motif chemokine ligand) 1 in ECs in an Lpar1/3-dependent manner.[12,13] Accordingly, blocking Lpar1/3 reduces atherosclerosis in mice.[12,14] Thus, mild LDL oxidation might induce the inflammatory activation of maladapted ECs by producing LPAs, in turn initiating and enhancing atherosclerosis.

In the extracellular space, LPAs are produced mainly by the secreted enzyme ENPP2 (ectonucleotide pyrophosphatase/phosphodiesterase 2; also known as autotaxin) through its lysophospholipase D activity.[15,16] More specifically, ENPP2 converts lysophospholipids, such as lysophosphatidylcholine (LPC), to LPAs.[17,18] Moreover, ENPP2 acts as a carrier protein for LPAs by providing a hydrophobic environment, efficiently delivering LPAs to their cognate receptors through binding to the cell surface.[15,19,20] Thus, ENPP2 not only produces LPAs but also regulates their signaling.[15,20] Notably, ENPP2 secreted from ECs increases the motility of lymphocytes and ECs by generating LPAs on the EC surface, indicating that it acts locally rather than systemically.[21] Inflammatory signaling, for example, by TNFα (tumor necrosis factor alpha), through the NF-κB (nuclear factor kappa light-chain enhancer of activated B cells) pathway upregulates the expression of ENPP2.[22,23] Moreover, LDL impairs angiogenesis by downregulating the endothelial expression of ENPP2 and production of LPAs.[24] In contrast, hyperlipidemia increases the levels of LPAs and activity of adipocyte-derived ENPP2 in the plasma.[25,26] Furthermore, the mildly oxidized LDL (moxLDL)–induced atherogenic adhesion of monocytes requires ENPP2 from the vascular wall, probably secreted from ECs.[12] However, whether endothelial ENPP2 contributes to atherosclerosis is not fully understood.

Our study showed that knockout of endothelial ENPP2 reduced atherosclerosis, macrophage recruitment, and endothelial expression of *Cxcl1* in *Apoe*$^{-/-}$ mice. This effect might have been due to the moxLDL-dependent generation of LPA16:0, LPA18:1, and LPA20:4 by EC-derived ENPP2. Thus, we assumed that endothelial ENPP2 plays a crucial role in atherosclerosis.

MATERIALS AND METHODS

The data that support the findings of this study are available from the corresponding author upon reasonable request.

Please see the Major Resources Table in the Supplemental Material.

Mouse Model

Mice harboring loxP-flanked *Enpp2* alleles (*Enpp2*$^{flox/flox}$) were crossed with *Apoe*$^{-/-}$ mice expressing tamoxifen-inducible Cre recombinase under the control of the EC-specific bone marrow X kinase promoter (BMX-Cre; *Apoe*$^{-/-}$*/BMX-Cre*$^{+}$*/Enpp2*$^{flox/flox}$ *C57Bl/6J*;EC-*Enpp2*$^{-/-}$).[27] BMX-Cre^{+} mice without *Enpp2* loxP-flanked alleles (*Apoe*$^{-/-}$*/BMX-Cre*$^{+}$*/Enpp2*$^{wt/wt}$; EC-*Enpp2*$^{+/+}$) were used as controls. Tamoxifen (2 mg per 20 g of body weight; Sigma-Aldrich Chemie GmbH, Taufkirchen, Germany) dissolved in medium-chain triglycerides (Miglyol 812; Caesar & Loretz GmbH, Hilden, Germany) was intraperitoneally injected in mice for 5 consecutive days. Seven days after

the last injection, the mice were fed a high-fat diet (HFD) containing 21% fat, 19.5% casein, and 0.15% cholesterol (ssniff Spezialdiäten GmbH, Soest, Germany) for 12 weeks. Blood was taken from the retro-orbital plexus and incubated with 200 U/mL lepirudin. Following centrifugation at 2.000*g* for 20 minutes, plasma was transferred to siliconized microcentrifuge tubes (Sigma-Aldrich). All animal experiments were approved by local authorities (District Government of Upper Bavaria) to comply with the German animal protection laws.

Immunostaining

After antigen retrieval using citrate buffer, aortic root sections were reacted with anti-Mac2 antibodies (clone M3/38; Cedarlane, Burlington, Canada), anti–α-SMA (smooth muscle actin) antibodies (1:200; clone 1A4; Agilent Technologies, Santa Clara, CA), anti-CD3 (clusters of differentiation) antibodies (1:100; Bio-Rad Laboratories GmbH, Feldkirchen, Germany), anti–von Willebrand Factor antibodies (1:1000; Abcam, Cambridge, United Kingdom), anti-CD31 antibodies (1:75; M20; Santa Cruz Biotechnology, Santa Cruz, CA), anti-Cxcl1 antibodies (ab86436; Abcam), anti–Ly-6G/Ly-6C antibodies (RB6-8C5; 1:50; eBioscience), and anti-Ki67 antibodies (ab15580; 1:1500; Abcam). Mac2 immunostaining was combined with terminal deoxynucleotidyl transferase dUTP nick end labeling assay (Roche). ENPP2 was detected in cryosections of the aortic roots fixed with BD Cytofix Fixation Buffer (BD Biosciences, Heidelberg, Germany) and in longitudinal sections of aortae fixed with PAXgene (Qiagen), after cooking in citrate buffer, with polyclonal rabbit anti-ENPP2 antibodies (PA5-12478; Thermo Fisher Scientific, Waltham, MA). Primary antibodies were detected after incubation with DyLight-488–conjugated, DyLight-550–conjugated, DyLight-650–conjugated (Abcam), or FITC/Cy3-conjugated (Jackson ImmunoResearch, Cambridgeshire, United Kingdom) secondary antibodies. Additional sections on the same slide were incubated with the appropriate IgG controls (Santa Cruz Biotechnology), followed by incubation with secondary antibodies. Nuclei were counterstained with 4′,6-diamidino-2-phenylindole. Images were recorded using a fluorescence microscope (DM6000B) connected to a monochrome digital camera (DFC365FX). The Mac2 and α-SMA positive area was quantified as a percentage of the plaque area, and $CD3^+$ cells were quantified as a percentage of all plaque cells using the ImageJ software (https://imagej.nih.gov).

Quantitative Real-Time PCR

Total RNA was extracted using the NucleoSpin RNA kit (Macherey-Nagel, Dueren, Germany). Reverse transcription was performed using a high-capacity cDNA reverse transcription kit (Thermo Fisher Scientific). Transcripts of mRNAs were amplified using specific primers (Table S1) and GoTaq qPCR Master Mix (Promega, Fitchburg, WI) and quantified (7900HT PCR System; Applied Biosystems). *B2m* was used as a reference gene. The relative expression levels were normalized to a single gene, scaled to the sample with the lowest expression, and logarithmically transformed (Qbase Software; Biogazelle, Gent, Belgium).

Preparation of moxLDL and Native LDL

Human LDL (1 mg/Ml; Merck, Darmstadt, Germany) was dialyzed for 24 hours to remove EDTA using a D-tube dialyzer (Merck). The LDL was then incubated with 5 μM $CuSO_4$ (Merck) at 37 °C, and the degree of formation of conjugated diene during oxidation was monitored via spectrophotometry at 234 nm (UV-Vis module; Nanodrop). The reaction was stopped at the end of the lag phase when absorption started to increase exponentially (usually within 1 hour) by adding 10 μmol/L EDTA (Thermo Fisher Scientific).[28] Native LDL (nLDL) was obtained by applying the same protocol without adding $CuSO_4$. Finally, moxLDL and nLDL were passed through PD-10 desalting columns (Cytiva).

Statistical Analysis

Statistical analysis was performed using Prism 9.0 (GraphPad Software, San Diego, CA). Data are represented as the mean±SD. Data have been analyzed for normality and equal variances. Comparisons between 2 groups were performed using the unpaired parametric 2-tailed Student *t* test or multiple *t* tests with correction for multiple comparisons (Holm-Sidak). Comparisons between >2 groups were performed using a 1-way ANOVA followed by a post hoc analysis using the Dunnett test or Tukey test to correct for multiple comparisons or a Brown-Forsythe and Welch ANOVA test followed by an unpaired *t* test with Welch correction. Two-factor statistical analysis was performed using a 2-way ANOVA followed by Sidak multiple comparison test. Differences were considered statistically significant at $P<0.05$. The nonparametric Spearman correlation coefficient and *P* testing the null hypothesis that no correlation between the two variables exists was also calculated. Sample sizes between 3 and 5 are potentially a limitation for parametric statistical tests.

RESULTS

Effect of Endothelial ENPP2 on Its Activity and Levels of LPAs in the Plasma

Immunostaining analysis revealed the absence of ENPP2 in aortic ECs of EC-*Enpp2*$^{-/-}$ mice compared with EC-*Enpp2*$^{+/+}$ mice 7 days after the last injection of tamoxifen (Figure 1A). In contrast, ENPP2 in smooth muscle cells did not differ between the groups (Figure 1A). Additionally, the level of expression of *Enpp2* was reduced in aortic ECs from EC-*Enpp2*$^{-/-}$ mice compared with those from EC-*Enpp2*$^{+/+}$ mice fed an HFD for 4 weeks (Figure 1B).

We observed that knocking out of endothelial *Enpp2* did not substantially alter the activity of plasma ENPP2 (Figure 1C) or plasma levels of LPAs (Figure 1D) in male and female mice after 12 weeks of HFD feeding. In contrast to the level of LPAs, we determined that the ENPP2 activity was higher in male compared with female EC-*Enpp2*$^{+/+}$mice and EC-*Enpp2*$^{-/-}$ mice (Figure 1C and 1D). Accordingly, a strong negative correlation was detected between the activity of plasma ENPP2 and total level of plasma LPA levels in EC-*Enpp2*$^{+/+}$mice (Figure 1E). This negative correlation was weaker in EC-*Enpp2*$^{-/-}$ mice (Figure 1E).

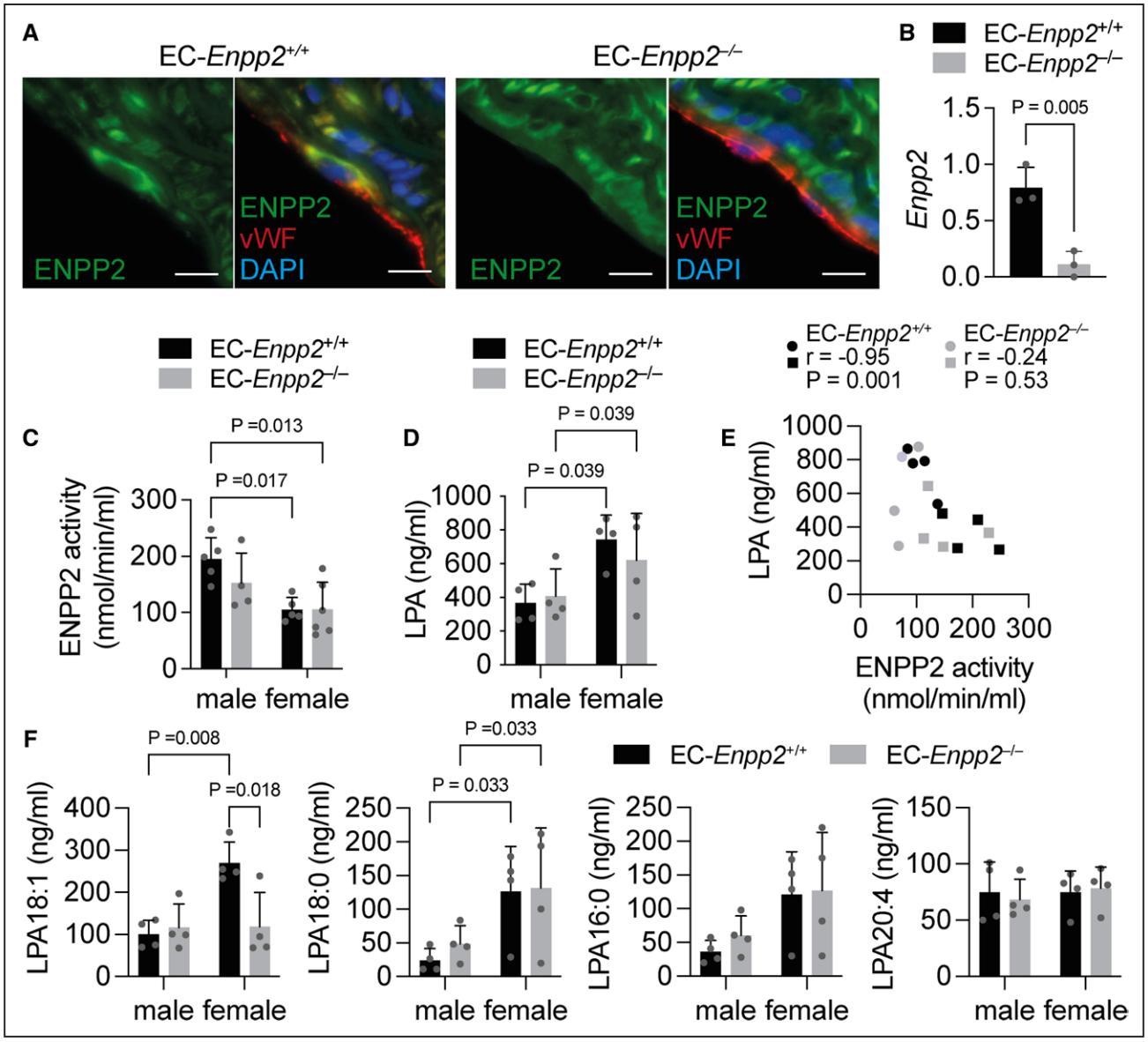

Figure 1. Effect of endothelial ENPP2 (ectonucleotide pyrophosphatase/phosphodiesterase 2) on the ENPP2/lysophosphatidic acid (LPA) axis in the plasma of *Apoe*$^{-/-}$ mice.

A, Expression of ENPP2 in the aortic root of endothelial cell (EC)–*Enpp2*$^{+/+}$ and EC-*Enpp2*–/– mice at day 7 after the last injection of tamoxifen (TMX) as determined by ENPP2 and VWF (von Willebrand Factor) immunostaining. Scale bars, 10 µm. Nuclei were counterstained using 4′,6-diamidino-2-phenylindole (DAPI). **B**, Level of expression of *Enpp2* mRNA in ECs isolated from aortae of EC-*Enpp2*$^{+/+}$ and EC-*Enpp2*$^{-/-}$ mice fed a high-fat diet (HFD) for 4 weeks as determined by qRT-PCR (real-time quantitative polymerase chain reaction; n=3 mice per group). Activity of ENPP2 (**C**; n=4–6 mice per group), concentration of total LPAs (**D**; n=4 mice per group), and correlation between the activity of ENPP2 and levels of total LPAs (**E**; n=8 mice per group; circles, females; rectangles, males) in the plasma of EC-*Enpp2*$^{+/+}$ and EC-*Enpp2*$^{-/-}$ mice fed the HFD for 12 weeks. **F**, Plasma levels of LPA species in EC-*Enpp2*$^{+/+}$ and EC-*Enpp2*$^{-/-}$ mice fed the HFD for 12 weeks (n=4 mice per group). Error bars indicate SD. Unpaired Student *t* test (**B**) and 2-way ANOVA with multiple comparison correction using the Sidak method (**C**, **D**, and **F**). Spearman correlation coefficient (r) was calculated (**E**).

Next, we investigated the effect of endothelial ENPP2 on the plasma levels of LPAs. We found that LPA18:1 and LPA18:2 were the most abundant LPA species in the plasma of male EC-*Enpp2*$^{+/+}$mice (Figure S1A), whereas the plasma level of LPA18:1 was higher than the other LPAs in female mice (Figure 1F; Figure S1B). Knocking out *Enpp2* reduced the level of LPA18:1 by 50% in female but not in male mice (Figure 1F). The level of LPA18:0 was higher in females than in male EC-*Enpp2*$^{+/+}$mice and EC-*Enpp2*$^{-/-}$ mice, but knocking out *Enpp2* did not alter its level in the plasma (Figure 1F). Similarly, the level of LPA16:0 tended to be higher in females; however, the difference was not statistically significant (Figure 1F). Moreover, the levels of LPA18:3 and LPA20:0 in male mice tended to be reduced by knocking out *Enpp2* without reaching statistical significance (Figure S2). We observed similar levels of LPA18:2 (Figure S2) and LPA20:4 (Figure 1F)

in female and male mice, and these were not altered by the endothelial *Enpp2* knockout.

We analyzed the effect of endothelial ENPP2 on the correlation between the activity of ENPP2 and the levels of individual LPA species in the plasma. We detected that the strong negative correlation between the activity of ENPP2 and the levels of LPA16:0, LPA18:0, and LPA18:1 in EC-*Enpp2*$^{+/+}$mice (Figure 2A) was absent in EC-*Enpp2*$^{-/-}$ mice (Figure 2B). In contrast, knocking out endothelial *Enpp2* did not alter the strong correlations between LPA16:0 and LPA18:0 and LPA18:2 and LPA18:3 (Figure 2). The level of LPA20:4 was not correlated with the plasma activity of ENPP2 in EC-*Enpp2*$^{+/+}$ (Figure 2A) and EC-*Enpp2*$^{-/-}$ mice (Figure 2B). Interestingly, the level of LPA18:1 was moderately correlated with the levels of LPA16:0 and LPA18:0 but not with those of LPA18:2, LPA18:3, LPA20:0, and LPA20:4 in EC-*Enpp2*$^{+/+}$ (Figure 2A) and EC-*Enpp2*$^{-/-}$ mice (Figure 2B). These results indicated that endothelial ENPP2 expression generates a negative correlation between the activity of plasma ENPP2 and the plasma levels of LPA16:0, LPA18:0, and LPA18:1.

Endothelial ENPP2 and Atherosclerosis

Next, we investigated the role of endothelial ENPP2 in atherosclerosis after 12 weeks of HFD feeding. We found that ENPP2 was detectable in ECs covering atherosclerotic lesions and in lesional macrophages in EC-*Enpp2*$^{+/+}$ mice (Figure 3A). Knocking out endothelial *Enpp2* decreased the plaque and necrotic core area in aortic roots in both sexes (Figure 3B). Furthermore, the Oil Red O–stained area in the aortic arch of male (Figure 3C) and female (Figure 3D) mice was reduced in EC-*Enpp2*$^{-/-}$ compared with EC-*Enpp2*$^{+/+}$ mice, whereas the size of lesions in the thoracic and abdominal aortae did not differ between groups (Figure 3C and 3D). These findings indicated that endothelial ENPP2 plays a proatherogenic role in both sexes.

We detected higher plasma levels of cholesterol in females than in male EC-*Enpp2*$^{+/+}$ mice (Figure 3E). This sex-related difference was not detected in EC-*Enpp2*$^{-/-}$ mice (Figure 3E). Moreover, the endothelial *Enpp2* knockout did not significantly affect the levels of cholesterol in either sex (Figure 3E). Although the correlation between the levels of cholesterol and plaque size was strong in EC-*Enpp2*$^{+/+}$ mice (Figure 3F), it was moderate in EC-*Enpp2*$^{-/-}$ mice (Figure 3G).

The EC-specific *Enpp2* knockout reduced the lesional content of macrophages but not smooth muscle cells in female and male mice (Figure 4A). More specifically, knocking out endothelial ENPP2 decreased the proliferation of macrophages (Figure 4B) and reduced the number of Ly6G (lymphocyte antigen 6 complex locus G6)+ monocytes adhering to the surface of aortic root lesions (Figure 4C) in both sexes. We did not detect any differences in the apoptosis of macrophages (Figure S3) and the CD3$^+$ T-cell content (Figure S4) between EC-*Enpp2*$^{-/-}$ and EC-*Enpp2*$^{+/+}$ mice in either sex. These data suggested that endothelial ENPP2 promotes atherosclerosis primarily by enhancing the recruitment of monocytes and the proliferation of macrophages.

The effect of endothelial ENPP2 on the inflammatory activation of aortic ECs was investigated. After 4 weeks of HFD feeding, the levels of expression of *Cxcl1* and *Ccl5* were reduced in aortic ECs from EC-*Enpp2*$^{-/-}$ mice compared with those in EC-*Enpp2*$^{+/+}$ mice (Figure 4D). Whereas the levels of expression of *Ccl2* and *Cx$_3$cl1* did not differ between the two groups, the level of expression of *Cxcl12* was higher in ECs from EC-*Enpp2*$^{-/-}$ mice than that in ECs from EC-*Enpp2*$^{+/+}$ mice (Figure 4D). In addition, the mRNA levels of expression of the Lpar1, Lpar2, and Lpar4 LPA receptors and those of *Icam1* and *Vcam1* were not different in the ECs between the two groups (Figure S5). Furthermore, the number of CXCL1-expressing ECs in the aortic root were lower in EC-*Enpp2*$^{-/-}$ mice than that in EC-*Enpp2*$^{+/+}$ mice after 12 weeks of HFD feeding, as determined by combined CXCL1 and CD31 immunostaining (Figure 4E). Thus, endothelial ENPP2 promotes endothelial inflammation by upregulating the expression of CXCL1.

Effect of ENPP2 on Endothelial Expression of Chemokines

We then investigated the mechanism by which endothelial ENPP2 regulates the expression of chemokines in vitro. Immunostaining and 3-dimensional confocal microscopy analysis revealed the presence of ENPP2 on the surface of murine aortic ECs (MAECs; Figure 5A). We found that stimulation of MAECs with the atherogenic cytokine TNFα, which triggers the secretion of ENPP2 from cancer cells,[23] increased the ENPP2 signal on the cell surface (Figure 5A). Live-cell imaging analysis of the activity of ENPP2 in TNFα-stimulated MAECs using the fluorogenic ENPP2 substrate FS-3 showed a time-dependent increase of FS-3 hydrolysis on the endothelial surface, resulting in the diffusion of the product (Figure 5B). These findings indicated that ENPP2 deposited on the EC surface can locally produce LPAs.

Next, we investigated the effect of ENPP2 on the expression of chemokines in MAECs. We observed that treatment with moxLDL or oxidized LDL (oxLDL) increased the expression of *Enpp2* mRNA in MAECs compared with nLDL (Figure 5C). Moreover, compared with nLDL, moxLDL increased the expression of *Cxcl1* (Figure 5D). We also found that blocking ENPP2 by S32826 decreased the expression of *Cxcl1* in moxLDL-treated but not in nLDL-treated MAECs (Figure 5D). In contrast, treatment with S32826 did not affect the levels of expression of *Ccl5* and *Cxcl12* in nLDL-treated or moxLDL-treated MAECs (Figure 5D).

To determine which LPAs regulate the expression of chemokines in ECs, we treated MAECs with LPA20:4, LPA16:0, and LPA18:1. Treatment with LPA20:4, LPA16:0, and LPA18:1 induced the expression of *Cxcl1*,

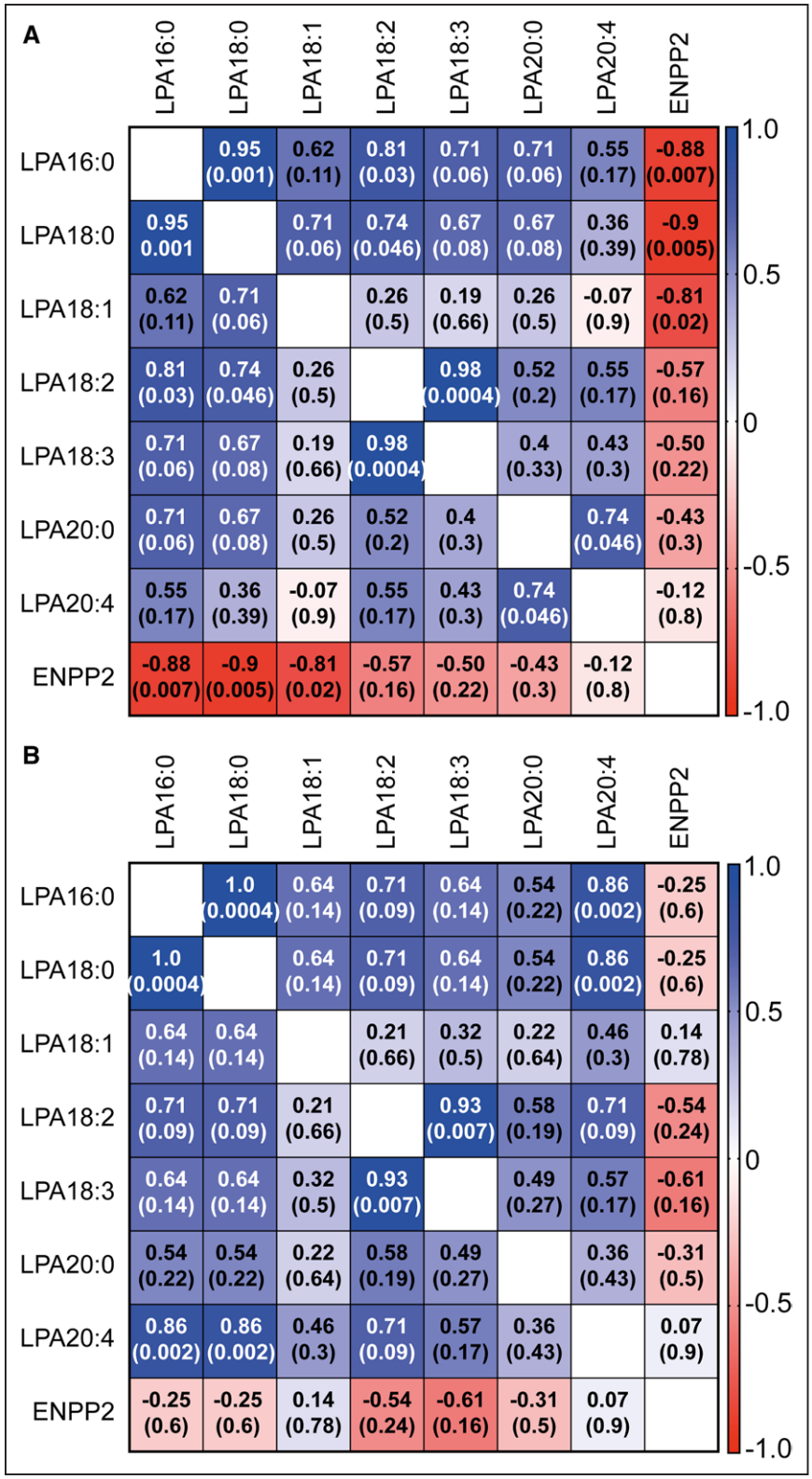

Figure 2. Effect of endothelial ENPP2 (ectonucleotide pyrophosphatase/phosphodiesterase 2) on the correlation between lysophosphatidic acid (LPA) species and ENPP2 activity.
Color-coded correlation matrix showing the Spearman correlation coefficient r between the levels of the LPA species and activity of ENPP2 measured in the plasma of endothelial cell (EC)–*Enpp2*$^{+/+}$ (**A**; n=8 mice per group) and EC-*Enpp2*$^{-/-}$ mice (**B**; n=8 mice per group) fed the high-fat diet for 12 weeks. The *P* values are displayed in brackets.

compared with the control buffer (Figure 5E). In contrast to LPA20:4, which did not significantly alter their expression, LPA16:0 and LPA18:1 upregulated both *Ccl5* and *Cxcl12* (Figure 5E). Furthermore, compared with nLDL, treatment with moxLDL increased the level of LPA16:0, whereas it reduced that of LPA20:4 (Figure 5F) and LPA20:0 (Figure S6) in the medium of MAECs. S32826 treatment decreased LPA16:0 and LPA20:4 concentrations in the medium of nLDL- and moxLDL-treated MAECs (Figure 5F). Whereas the level of LPA18:1 in the medium of nLDL-treated MAECs varied greatly, treatment with moxLDL resulted in an ENPP2-dependent

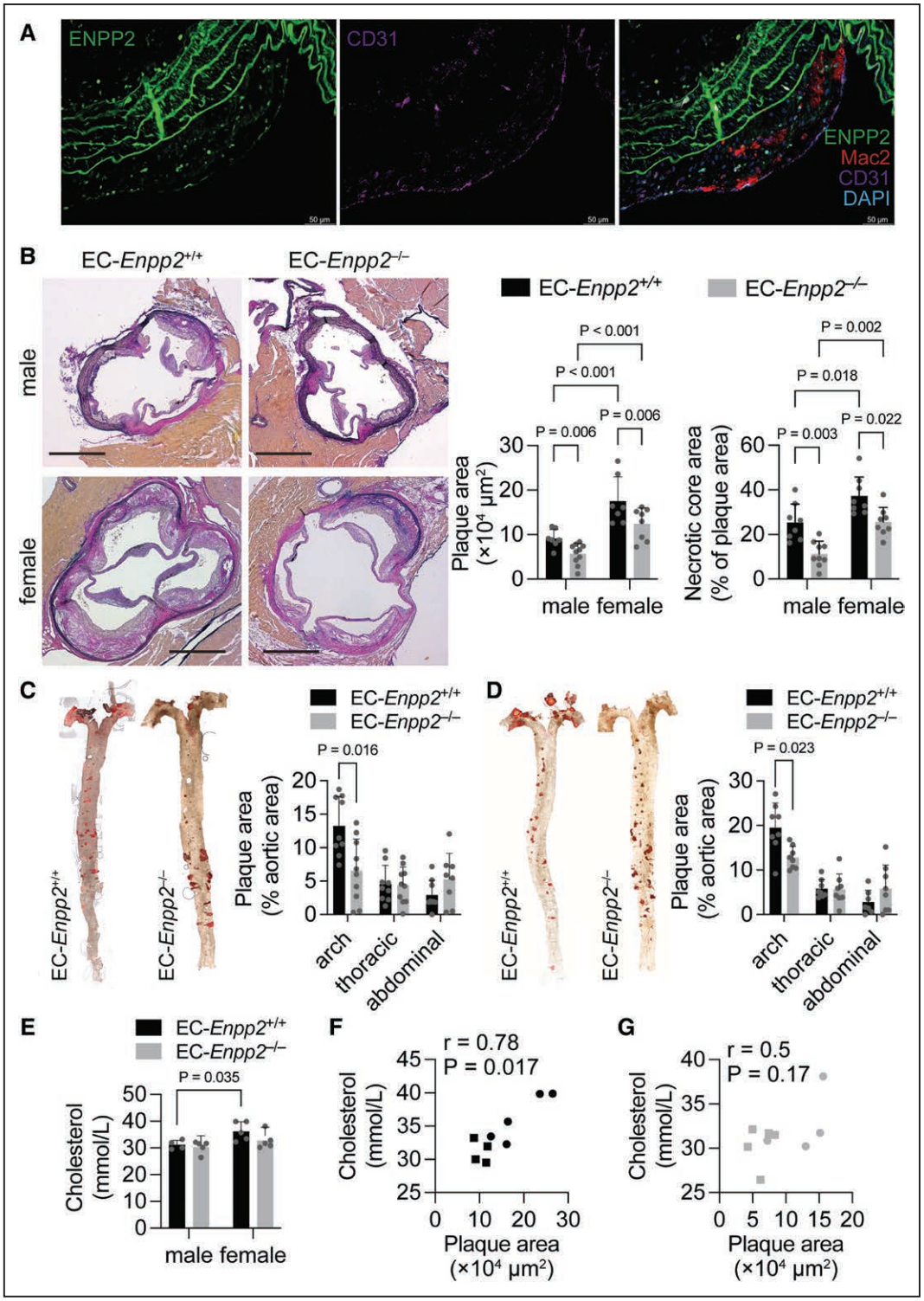

Figure 3. Effect of endothelial ENPP2 (ectonucleotide pyrophosphatase/phosphodiesterase 2) on atherosclerosis.
A, Combined ENPP2, CD31 (clusters of differentiation), and Mac2 immunostaining in longitudinal sections of the aortic arch from *Apoe*$^{-/-}$ mice after 12 weeks of high-fat diet feeding. Scale bars, 50 µm. **B**, Plaque and necrotic core areas were determined in the aortic roots of mice (n=7–10 mice per group). Representative images of aortic root sections stained with Elastic van Gieson are shown. Scale bars, 500 µm. **C** and **D**, Quantification of the lipid deposition in plaques of the aorta determined by Oil red O staining of en face prepared aortae. Representative images are shown. The plaque area in the aortic arch and the thoracic and abdominal aorta is presented as a percentage of the whole aortic area in male (**C**; n=8–10 mice per each group) and female (**D**; n=7–8 mice per each group) endothelial cell (EC)–*Enpp2*$^{+/+}$ and EC-*Enpp2*$^{-/-}$ mice. **E**, Plasma levels of cholesterol and the correlation between the levels of cholesterol and plaque size in EC-*Enpp2*$^{+/+}$ (**F**) and EC-*Enpp2*$^{-/-}$ mice (**G**). Spearman correlation coefficient *r* was calculated (**F** and **G**). Circles, female mice; rectangles, male mice. Multiple *t* tests and multiple comparison correction using the Holm-Sidak method (**C** and **D**) and 2-way ANOVA followed by Sidak multiple comparison correction (**B** and **E**). Error bars indicate SD.

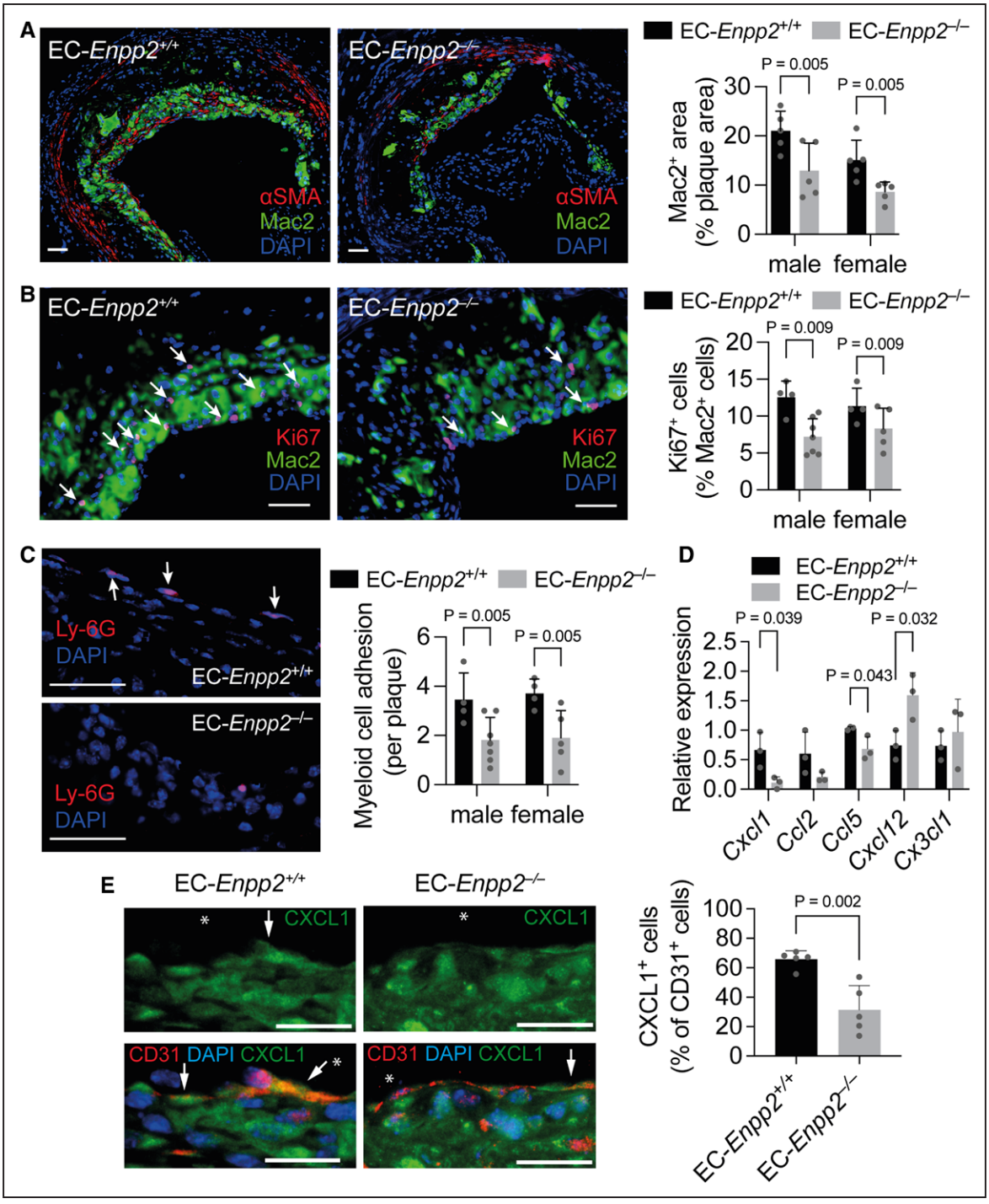

Figure 4. Endothelial Enpp2 (ectonucleotide pyrophosphatase/phosphodiesterase 2) knockout affects accumulation of lesional macrophages.

Aortic root sections from endothelial cell (EC)–*Enpp2*$^{+/+}$ and EC-*Enpp2*$^{-/-}$ mice fed the high-fat diet (HFD) for 12 weeks were analyzed. **A**, Quantification of the macrophage area normalized to the plaque area as determined by Mac2 immunostaining (n=5 mice per group). **B**, Quantification of macrophage proliferation by combined Ki67 and Mac2 immunostaining (n=4–7 mice per group). **C**, Adhesion of myeloid cells to the plaque surface quantified in aortic root sections immunostained with Ly-6G antibodies (n=4–7 mice per group). **A** through **C**, Nuclei were counterstained with 4′,6-diamidino-2-phenylindole (DAPI). Scale bars, 50 µm. **D**, Expression of chemokines quantified by qPCR (real-time quantitative polymerase chain reaction) in aortic ECs isolated in nitrocellulose membrane from EC-*Enpp2*$^{+/+}$ and EC-*Enpp2*$^{-/-}$ mice after injection of tamoxifen (TMX) and 4 weeks of HFD feeding (n=3 mice per group). **E**, Percentage of CXCL (C-X-C motif chemokine ligand) 1–expressing CD31^{+} (clusters of differentiation) ECs in aortic root lesions of EC-*Enpp2*$^{+/+}$ and EC-*Enpp2*$^{-/-}$ mice (n=5 mice per group) after 12 weeks of HFD feeding as determined by combined CXCL1 and CD31 immunostaining. Arrows indicate CXCL1^{+} ECs. Asterisks indicate the vessel lumen. Nuclei were counterstained with DAPI. Scale bars, 25 µm. Two-way ANOVA followed by Sidak multiple comparison correction (**A**–**C**) and Student *t* tests (**D** and **E**) and multiple comparison correction using the Holm-Sidak method (**D**). Error bars indicate SD.

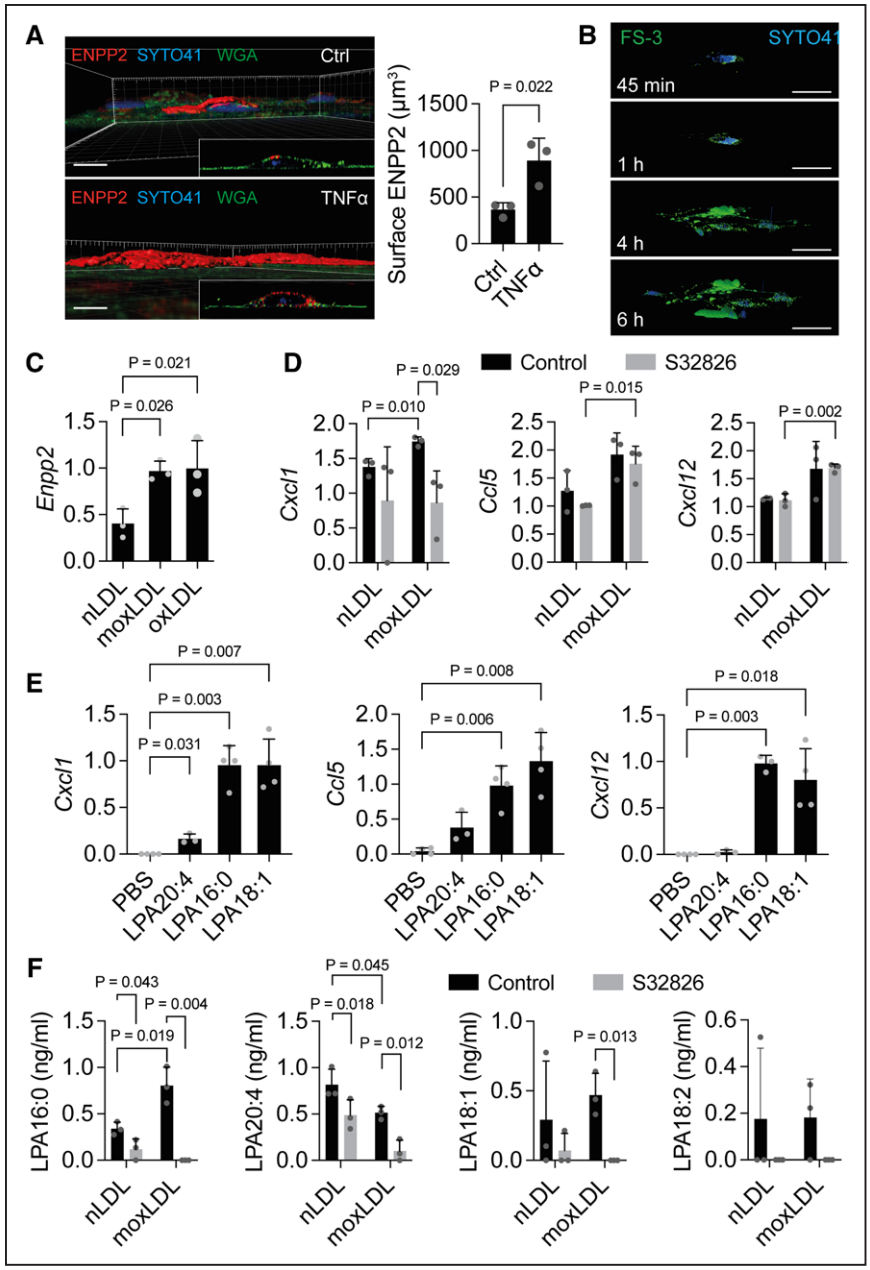

Figure 5. Activity of endothelial ENPP2 (ectonucleotide pyrophosphatase/phosphodiesterase 2) and expression of chemokines. **A**, Surface deposition of ENPP2 on murine aortic endothelial cells (MAECs) treated with control buffer (Ctrl) or TNFα (tumor necrosis factor alpha) was determined by ENPP2 immunostaining and confocal microscopy. Images are 3-dimensional reconstructions of z stacks. The cell membrane was stained using WGA (wheat germ agglutinin). Scale bars, 7 µm. **B**, Three-dimensional live-cell imaging of the activity of ENPP2 in TNFα-stimulated MAECs treated with the fluorogenic ENPP2 substrate FS-3. Z stacks of confocal microscopy images were used for 3-dimensional reconstruction. Nuclei were counterstained with SYTO41. Scale bars, 50 µm. **C**, Expression of *Enpp2* mRNA in MAECs treated with native LDL (nLDL), mildly oxidized LDL (moxLDL), and oxidized LDL (oxLDL; n=3 replicates per group). **D**, Expression of chemokines determined by qPCR (real-time quantitative polymerase chain reaction) in nLDL- or moxLDL-stimulated MAECs treated with or without the ENPP2 inhibitor S32826 (n=3 biological replicates). **E**, Level of expression of chemokines in MAECs treated with different lysophosphatidic acid (LPA) species (10 µg/mL for 6 h) as determined by qPCR (n=3–4 replicates per group). **F**, Concentration of different LPA species quantified by mass spectrometry in the medium of MAECs (n=3) treated with moxLDL or nLDL with or without S32826. Student *t* test (**A** and **D**), 1-way ANOVA and Dunnett multiple comparisons test (**C**), Brown-Forsythe and Welch ANOVA test followed by unpaired *t* test using Welch correction (**E**), and multiple *t* tests with multiple comparison correction using the Holm-Sidak method (**F**). Error bars indicate SD.

production of LPA18:1 (Figure 5F). In contrast to mox-LDL, nLDL-treated MAECs produced LPA20:0 in an ENPP2-dependent manner (Figure S6). We detected LPA18:0 only in one replicate of moxLDL-treated MAECs (Figure S6), while LPA18:3 was not measurable in any of the groups (data not shown). Thus, moxLDL-induced upregulation of ENPP2 in ECs might increase the expression of CXCL1 through the generation of LPAs, such as LPA16:0, LPA18:1, and LPA20:4.

Endothelial ENPP2 and the Correlation Between the Plasma LPA/ENPP2 Axis and Plaque Size

We further investigated the effect of endothelial ENPP2 on the correlation between the plasma LPA/ENPP2 axis and atherosclerosis. Notably, the total levels of LPAs and the activity of ENPP2 in the plasma showed a strong positive and negative correlation, respectively, with plaque size in EC-*Enpp2*$^{+/+}$ mice (Figure 6A). However, these contrary correlations were weaker and did not reach statistical significance in EC-*Enpp2*$^{-/-}$ mice (Figure 6B). Furthermore, the plasma levels of LPA16:0 (Figure 6C) and LPA18:0 (Figure 6D) were almost perfectly correlated with the plaque size in EC-*Enpp2*$^{+/+}$ mice; however, the correlation between those LPAs and plaque size was only moderate and not statistically significant in EC-*Enpp2*$^{-/-}$ mice (Figure 6C and 6D). The strong positive correlation between LPA18:1 plasma level and plaque size in EC-*Enpp2*$^{+/+}$ mice was absent in EC-*Enpp2*$^{-/-}$ mice (Figure 6E). In contrast, the moderate association between the plasma levels

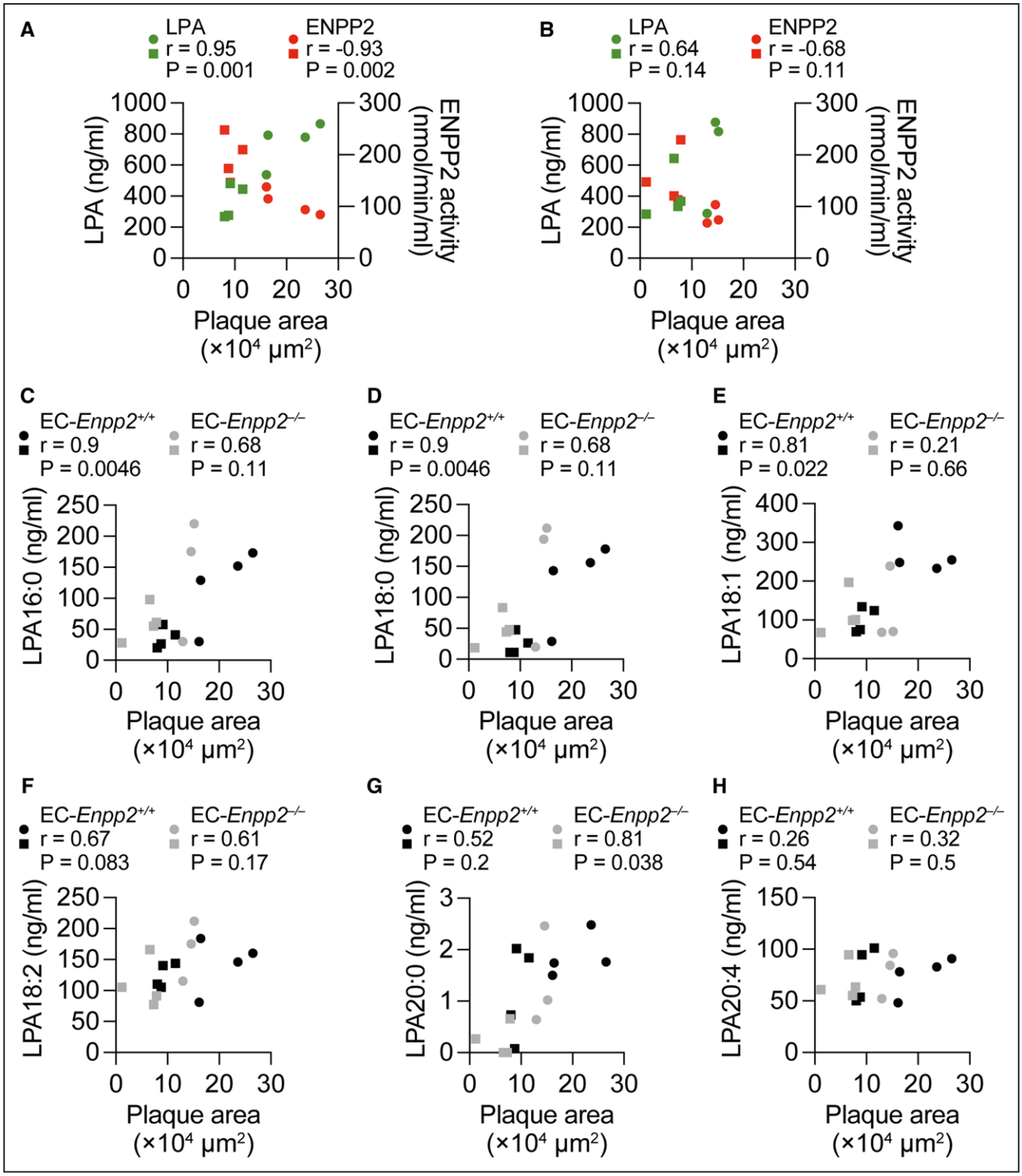

Figure 6. Endothelial ENPP2 (ectonucleotide pyrophosphatase/phosphodiesterase 2) regulates the relationship between the plasma ENPP2/lysophosphatidic acid (LPA) axis and atherosclerosis.
Correlation between the level of total LPAs or the activity of ENPP2 in the plasma with the size of the plaques in endothelial cell (EC)–*Enpp2*$^{+/+}$ mice (**A**) and EC-*Enpp2*–/– mice (**B**). **C** through **H**, Correlation between the plasma level of the LPA species and plaque size. Spearman correlation coefficient (r) was calculated. Circles, female mice; rectangles, male mice.

of LPA18:2 (Figure 6F) and LPA18:3 (Figure S7) and plaque size in EC-*Enpp2*$^{+/+}$ mice was not substantially altered by knocking out endothelial *Enpp2*. Notably, only the association between the level of LPA20:0 and plaque size was stronger in EC-*Enpp2*$^{-/-}$ than in EC-*Enpp2*$^{+/+}$ mice (Figure 6G). The plasma levels of LPA20:4 were not associated with plaque size either in EC-*Enpp2*$^{+/+}$ or EC-*Enpp2*$^{-/-}$ mice (Figure 5H). These

results indicated that endothelial ENPP2 determines the association of circulating levels of LPA16:0 and LPA18:0 with atherosclerosis.

Endothelial ENPP2 and the Regulation of Body Weight During HFD Feeding

We specifically observed that in contrast to female mice, knocking out endothelial *Enpp2* increased the body weight of male *Apoe*$^{-/-}$ mice (Figure 7A). Although the correlation between the activity of plasma ENPP2 and body weight of EC-*Enpp2*$^{+/+}$ and EC-*Enpp2*$^{-/-}$ mice did not reach statistical significance, the endothelial *Enpp2* knockout changed the Spearman correlation coefficient from positive to negative (Figure 7B). In contrast, the plasma levels of LPAs, LPA16:0, LPA18:0, LPA18:2, and LPA18:3 were positively correlated with the body weight of the HFD-fed EC-*Enpp2*$^{+/+}$ mice (Figure 7C and 7D). The correlation between the levels of total LPA, LPA16:0, and LPA18:0 and body weight could be fitted to a sinus wave (Figure 7C and 7D), indicating a sigmoid correlation. However, the strong positive correlation between LPA18:2 and LPA18:3 with weight was linear (Figure 7D). Notably, knocking out endothelial *Enpp2* reversed, although not in a statistically significant manner, the positive correlation between the levels of LPA18:2 and weight observed in EC-*Enpp2*$^{+/+}$ mice (Figure 7D). Interestingly, the plasma levels of total LPA, LPA16:0, LPA18:0, and LPA18:3 were not correlated with body weight in EC-*Enpp2*$^{-/-}$ mice (Figure 7C and 7D). In contrast, the plasma levels of LPA20:0 were negatively correlated with body weight in EC-*Enpp2*$^{-/-}$ mice (Figure 7D). Compared with other LPA species, the plasma levels of LPA20:4 were not associated with body weight in EC-*Enpp2*$^{+/+}$ and EC-*Enpp2*$^{-/-}$ mice (Figure S8). These findings indicated that the activity of endothelial ENPP2 regulates the correlation between the level of circulating LPA species, such as LPA18:2 and LPA18:3, and body weight.

DISCUSSION

Our study demonstrated that knocking out endothelial *Enpp2* reduces atherosclerosis in *Apoe*$^{-/-}$ mice in a sex-independent manner due to reduced accumulation of lesional macrophages. Furthermore, ENPP2 from ECs generated LPAs, such as LPA16:0, LPA18:1, and LPA20:4, which promoted the moxLDL-induced expression of endothelial *Cxcl1*, thus potentially increasing the adhesion of monocytes and accumulation of macrophages. Moreover, endothelial ENPP2 established a strong correlation between plasma levels of LPAs, such as LPA16:0 and LPA18:0, and the plaque size, indicating that they play a role in atherosclerosis.

We previously determined that the vessel wall–derived activity of ENPP2 promoted the moxLDL-mediated adhesion of monocytes by upregulating CXCL1 in ECs.[12,13] This effect was attributed to the generation of LPA20:4 from LPC substrates obtained during the mild oxidation of LDL.[8,29] Accordingly, treatment with LPA20:4 increases atherosclerosis and the CXCL1-mediated adhesion of monocyte.[12] In line with these results, we showed that endothelial ENPP2 enhanced the formation of plaques, adhesion of monocytes, and expression of endothelial CXCL1. Therefore, we believe that endothelial ENPP2 increases atherosclerosis by CXCL1-mediated monocyte recruitment. In addition, our results would be compatible with the hypothesis that endothelial ENPP2 enhances macrophage proliferation by LPA-mediated upregulation of CXCL1.

Moreover, our results indicated that endothelial ENPP2 enhanced atherosclerosis by generating LPA16:0 and LPA18:1 because they were, similar to LPA20:4, effectively produced in the presence of moxLDL, strongly inducing the expression of *Cxcl1* in ECs. Interestingly, both LPA16:0 and LPA18:1 are known to be primarily accumulated in murine and human atherosclerotic lesions.[30,31] Furthermore, intestinal production of LPA18:1 has been associated with the formation of plaques.[32] ENPP2 also generated LPA16:0, LPA20:0, and LPA20:4 in the presence of nLDL. This finding is in agreement with studies demonstrating that ENPP2 produces LPA from LDL-associated substrates.[26] The differences between nLDL and moxLDL treatment in ENPP2-mediated LPA production may be due to the generation of specific LPCs during the oxidation of LDL.[29]

Notably, endothelial ENPP2 established a strong correlation between the plasma levels of LPA16:0, LPA18:0, and LPA18:1 and plaque size, suggesting that the production of these LPAs by EC-derived ENPP2 contributes to atherosclerosis. However, knocking out endothelial *Enpp2* did not affect the plasma levels of LPA16:0 and LPA18:0, probably because the activity of ENPP2 derived from other cell types compensates for the lack of the EC-dependent production of LPAs. Our results showed that ENPP2 is immobilized on the endothelial surface, where it locally hydrolyzed an LPC analog. As knocking out endothelial *Enpp2* did not affect the activity of plasma ENPP2, we believe that endothelial ENPP2-derived LPA16:0, LPA18:0, and LPA18:1 in the plasma might represent a spillover of the localized production of LPAs on the surface of ECs. Accordingly, secreted ENPP2 binds via integrins and heparan sulfate proteoglycans to cell membranes and supports localized signaling by presenting LPAs to their receptors.[15,20,33,34] Thus, the local accumulation of LPAs at the endothelial surface may play a role in plaque formation.

In contrast to previous studies in healthy humans,[35] the activity of ENPP2 was inversely correlated with the levels of LPA16:0 and LPA18:0 in the plasma of hyperlipidemic mice, indicating that the production of these LPAs by endothelial ENPP2 may limit the activity of plasma ENPP2. Although LPA16:0 can limit its

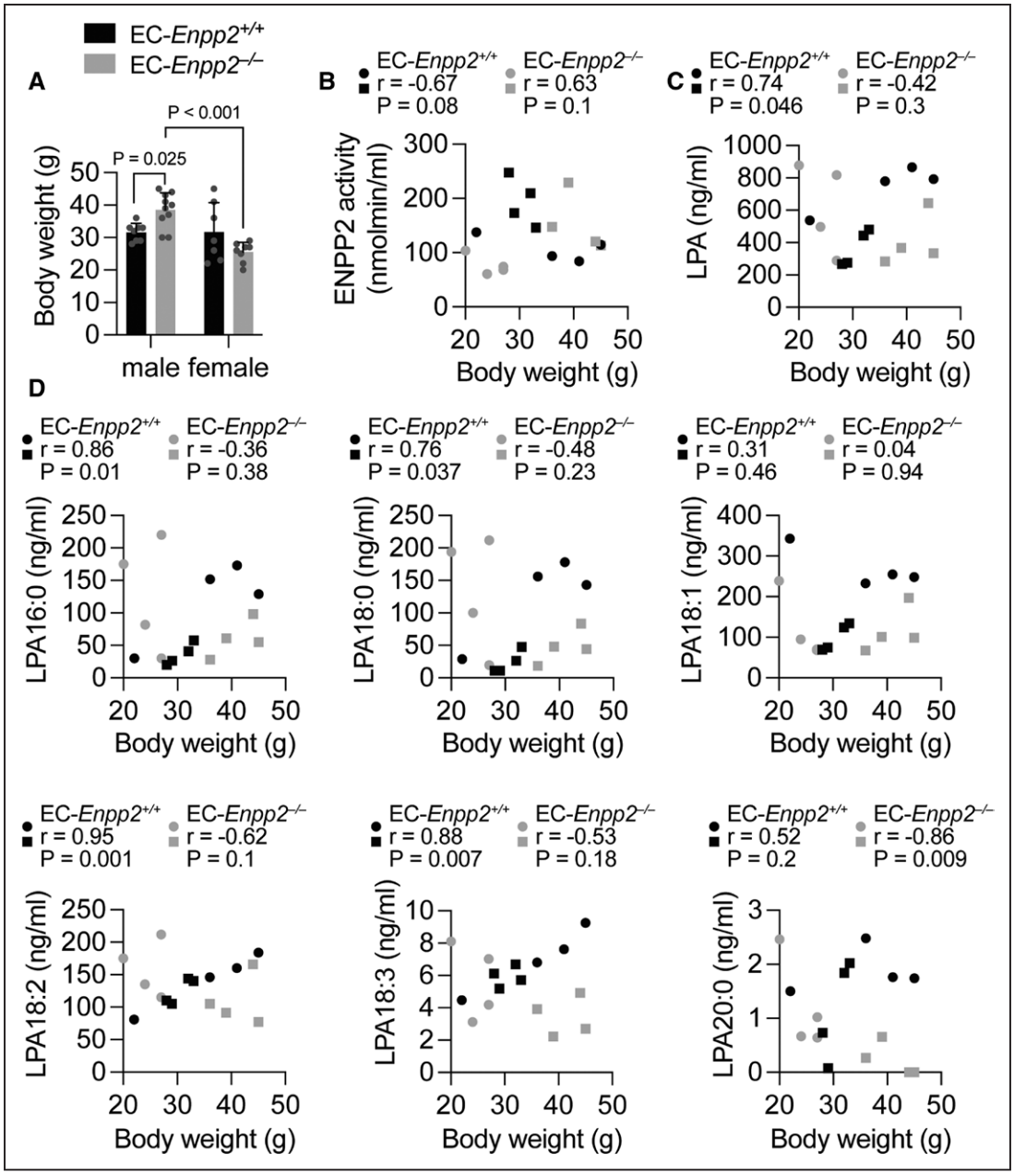

Figure 7. Endothelial ENPP2 (ectonucleotide pyrophosphatase/phosphodiesterase 2) limits body weight in male *Apoe*$^{-/-}$ mice. **A**, Body weight of endothelial cell (EC)–*Enpp2*$^{+/+}$ and EC-*Enpp2*$^{-/-}$ mice (n=7–10 mice per group) after 12 weeks of high-fat diet (HFD) feeding (2-way ANOVA and multiple comparison correction using the Sidak method). Correlation between activity of ENPP2 (**B**), level of total lysophosphatidic acids (LPAs; **C**), or the levels of the LPA species (**D**) and body weight after 12-week HFD feeding. Circles, female mice; rectangles, male mice. **B** through **D**, Spearman correlation coefficient (r) was calculated. Error bars indicate SD.

production by inhibiting the activity of ENPP2 in vitro,[36] the mechanism by which endothelial ENPP2 regulates the plasma ENPP2/LPA axis is not clear. In individuals harboring the SNP rs10757274 on chromosome 9p21, which increases the risk for coronary heart disease by 30% independent of traditional risk factors, the activity of plasma ENPP2 was uncoupled from the production of LPAs.[37] Thus, the inversion of the ENPP2/LPA ratio in the circulation might be representative of increased atherogenesis due to enhanced production of LPAs at the vessel wall.

In line with previous results,[38] female *Apoe*$^{-/-}$ mice developed larger and more advanced lesions than male mice after 12 weeks of HFD. This effect might have been, at least, in part, due to the higher plasma levels of cholesterol in female mice. Interestingly, the levels of cholesterol did not differ between male and female EC-*Enpp2*$^{-/-}$ mice, indicating that the production of LPAs by endothelial ENPP2 plays a sex-specific role in the regulation of the levels of cholesterol. Notably, intestinally derived LPA species increase the plasma levels of cholesterol in mice.[39] However, the mechanism by which

LPAs affect cholesterol and lipoprotein metabolism remains unclear.

Moreover, endothelial ENPP2 increased the plasma levels of LPA18:1 in female mice, which contributed substantially to the higher total plasma levels of LPAs compared with male mice. Accordingly, in humans, the total levels of LPAs are higher in women than in men.[40] The cause of this sex-specific effect of endothelial ENPP2 on the production of LPAs remains unclear. One possibility is that the substrate of ENPP2 differs between male and female mice because of the sex-specific composition of LPCs in plasma and VLDL (very-low–density lipoprotein)—the primary lipoprotein in *Apoe*$^{-/-}$ mice.[41,42]

In addition, our study suggested that endothelial ENPP2 regulates body weight by generating LPAs during HFD feeding based on 2 effects following the knockout of endothelial ENPP2: reduced correlation between several LPA species, in particular, between LPA18:2 and LPA18:3, with the body weight, and the increased weight of male *Apoe*$^{-/-}$ mice after the HFD period. Although *Apoe*$^{-/-}$ mice gain weight during HFD feeding mainly by increasing their adipose tissue mass,[43] they are, in contrast to C57Bl/6 and *Ldlr*$^{-/-}$ mice, protected from obesity due to reduced triglyceride uptake by adipocytes.[44–46] Therefore, the effect of endothelial ENPP2 on the correlation between the LPA species and weight is not indicative of a role of endothelial ENPP2 and LPAs in obesity.[47] Our results correlated with the concept that weight gain of lean HFD-fed mice increased the generation of LPA species, such as LPA18:2 and LPA18:3, by endothelial ENPP2. The finding that endothelial *Enpp2* knockout in male mice increased their weight and reduced the plasma levels of LPA18:3 indicated that the localized production of LPA18:3 at the vessel wall limits weight gain. Therefore, a negative feedback regulation between weight and endothelial ENPP2-mediated production of LPA18:3 might be instrumental in male mice. Notably, ECs control weight gain and adipose tissue mass following HFD feeding by regulating lipoprotein and triglyceride homeostasis.[48,49]

In conclusion, we demonstrated that endothelial ENPP2 promotes atherosclerosis in both sexes, most likely by generating LPA species, such as LPA16:0, LPA18:1, and LPA20:4, which enhance endothelial inflammation. Therefore, targeting ENPP2 to limit endothelial inflammation and lesion progression represents a promising strategy for treating cardiovascular diseases.

ARTICLE INFORMATION

Received November 17, 2020; accepted June 1, 2022.

Affiliations

Institute for Cardiovascular Prevention, University Hospital, Ludwig-Maximilians-University, Munich, Germany (E.K., R.M., M.Z., F.Z., C.G., R.T.A.M., M.B., M.N.-J., A.S.). Institute of Clinical Pharmacology, Johann Wolfgang Goethe-University, Frankfurt, Germany (D.T., N.F.). Fraunhofer Institute for Translational Medicine and Pharmacology, Frankfurt, Germany (D.T.). Division of Immunology, Biomedical Science Research, Center Alexander Fleming, Athens, Greece (C.M., V.A.). Cardiovascular Research Institute Maastricht, Maastricht University, the Netherlands (M.Z., R.T.A.M.). German Centre for Cardiovascular Research, Partner Site Munich Heart Alliance, Germany (M.N.-J., A.S.).

Acknowledgments

The authors thank Kathrin Abschlag for her technical assistance.

Sources of Funding

This work was supported by the German Research Foundation (Deutsche Forschungsgemeinschaft) as part of the Collaborative Research Center 1123 (B08), awarded to (B08) A. Schober and (Z01) to R.T.A. Megens; grant number KA 4209/2-1 awarded to E. Karshovska; and the LOEWE (Landes-Offensive zur Entwicklung wissenschaftlicher-ökonomischer Exzellenz) initiative from the State of Hessen (Germany) "Anwendungsorientierte Arzneimittelforschung," awarded to D. Thomas and N. Ferreirós.

Disclosures

None.

Supplemental Material

Supplemental Materials and Methods
Figures S1–S8
Table S1
References 50,51

REFERENCES

1. Schober A, Maleki SS, Nazari-Jahantigh M. Regulatory non-coding RNAs in atherosclerosis. *Handb Exp Pharmacol*. 2022;270:463–492. doi: 10.1007/164_2020_423
2. Schober A, Nazari-Jahantigh M, Wei Y, Bidzhekov K, Gremse F, Grommes J, Megens RT, Heyll K, Noels H, Hristov M, et al. MicroRNA-126-5p promotes endothelial proliferation and limits atherosclerosis by suppressing Dlk1. *Nat Med*. 2014;20:368–376. doi: 10.1038/nm.3487
3. Levitan I, Volkov S, Subbaiah PV. Oxidized LDL: diversity, patterns of recognition, and pathophysiology. *Antioxid Redox Signal*. 2010;13:39–75. doi: 10.1089/ars.2009.2733
4. van Hinsbergh VW, Scheffer M, Havekes L, Kempen HJ. Role of endothelial cells and their products in the modification of low-density lipoproteins. *Biochim Biophys Acta*. 1986;878:49–64. doi: 10.1016/0005-2760(86)90343-7
5. Parthasarathy S, Wieland E, Steinberg D. A role for endothelial cell lipoxygenase in the oxidative modification of low density lipoprotein. *Proc Natl Acad Sci USA*. 1989;86:1046–1050. doi: 10.1073/pnas.86.3.1046
6. Furnkranz A, Schober A, Bochkov VN, Bashtrykov P, Kronke G, Kadl A, Binder BR, Weber C, Leitinger N. Oxidized phospholipids trigger atherogenic inflammation in murine arteries. *Arterioscler Thromb Vasc Biol*. 2005;25:633–638. doi: 10.1161/01.ATV.0000153106.03644.a0
7. Liao F, Berliner JA, Mehrabian M, Navab M, Demer LL, Lusis AJ, Fogelman AM. Minimally modified low density lipoprotein is biologically active in vivo in mice. *J Clin Invest*. 1991;87:2253–2257. doi: 10.1172/JCI115261
8. Siess W, Zangl KJ, Essler M, Bauer M, Brandl R, Corrinth C, Bittman R, Tigyi G, Aepfelbacher M. Lysophosphatidic acid mediates the rapid activation of platelets and endothelial cells by mildly oxidized low density lipoprotein and accumulates in human atherosclerotic lesions. *Proc Natl Acad Sci USA*. 1999;96:6931–6936. doi: 10.1073/pnas.96.12.6931
9. Mills GB, Moolenaar WH. The emerging role of lysophosphatidic acid in cancer. *Nat Rev Cancer*. 2003;3:582–591. doi: 10.1038/nrc1143
10. Kano K, Aoki J, Hla T. Lysophospholipid mediators in health and disease. *Annu Rev Pathol*. 2022;17:459–483. doi: 10.1146/annurev-pathol-050420-025929
11. Bandoh K, Aoki J, Taira A, Tsujimoto M, Arai H, Inoue K. Lysophosphatidic acid (LPA) receptors of the EDG family are differentially activated by LPA species. Structure-activity relationship of cloned LPA receptors. *FEBS Lett*. 2000;478:159–165. doi: 10.1016/s0014-5793(00)01827-5
12. Zhou Z, Subramanian P, Sevilmis G, Globke B, Soehnlein O, Karshovska E, Megens R, Heyll K, Chun J, Saulnier-Blache JS, et al. Lipoprotein-derived lysophosphatidic acid promotes atherosclerosis by releasing CXCL1 from the endothelium. *Cell Metab*. 2011;13:592–600. doi: 10.1016/j.cmet.2011.02.016
13. Akhtar S, Hartmann P, Karshovska E, Rinderknecht FA, Subramanian P, Gremse F, Grommes J, Jacobs M, Kiessling F, Weber C, et al. Endothelial

hypoxia-inducible factor-1α promotes atherosclerosis and monocyte recruitment by upregulating microRNA-19a. *Hypertension*. 2015;66:1220–1226. doi: 10.1161/HYPERTENSIONAHA.115.05886
14. Kritikou E, van Puijvelde GH, van der Heijden T, van Santbrink PJ, Swart M, Schaftenaar FH, Kröner MJ, Kuiper J, Bot I. Inhibition of lysophosphatidic acid receptors 1 and 3 attenuates atherosclerosis development in LDL-receptor deficient mice. *Sci Rep*. 2016;6:37585. doi: 10.1038/srep37585
15. Moolenaar WH, Perrakis A. Insights into autotaxin: how to produce and present a lipid mediator. *Nat Rev Mol Cell Biol*. 2011;12:674–679. doi: 10.1038/nrm3188
16. Schober A, Siess W. Lysophosphatidic acid in atherosclerotic diseases. *Br J Pharmacol*. 2012;167:465–482. doi: 10.1111/j.1476-5381.2012.02021.x
17. Magkrioti C, Galaris A, Kanellopoulou P, Stylianaki EA, Kaffe E, Aidinis V. Autotaxin and chronic inflammatory diseases. *J Autoimmun*. 2019;104:102327. doi: 10.1016/j.jaut.2019.102327
18. Zhang X, Li M, Yin N, Zhang J. The expression regulation and biological function of autotaxin. *Cells*. 2021;10:939. doi: 10.3390/cells10040939
19. Nishimasu H, Okudaira S, Hama K, Mihara E, Dohmae N, Inoue A, Ishitani R, Takagi J, Aoki J, Nureki O. Crystal structure of autotaxin and insight into GPCR activation by lipid mediators. *Nat Struct Mol Biol*. 2011;18:205–212. doi: 10.1038/nsmb.1998
20. Hausmann J, Kamtekar S, Christodoulou E, Day JE, Wu T, Fulkerson Z, Albers HM, van Meeteren LA, Houben AJ, van Zeijl L, et al. Structural basis of substrate discrimination and integrin binding by autotaxin. *Nat Struct Mol Biol*. 2011;18:198–204. doi: 10.1038/nsmb.1980
21. Nakasaki T, Tanaka T, Okudaira S, Hirosawa M, Umemoto E, Otani K, Jin S, Bai Z, Hayasaka H, Fukui Y, et al. Involvement of the lysophosphatidic acid-generating enzyme autotaxin in lymphocyte-endothelial cell interactions. *Am J Pathol*. 2008;173:1566–1576. doi: 10.2353/ajpath.2008.071153
22. Benesch MG, Zhao YY, Curtis JM, McMullen TP, Brindley DN. Regulation of autotaxin expression and secretion by lysophosphatidate and sphingosine 1-phosphate. *J Lipid Res*. 2015;56:1134–1144. doi: 10.1194/jlr.M057661
23. Wu JM, Xu Y, Skill NJ, Sheng H, Zhao Z, Yu M, Saxena R, Maluccio MA. Autotaxin expression and its connection with the TNF-alpha-NF-kappaB axis in human hepatocellular carcinoma. *Mol Cancer*. 2010;9:71. doi: 10.1186/1476-4598-9-71
24. Gibbs-Bar L, Tempelhof H, Ben-Hamo R, Ely Y, Brandis A, Hofi R, Almog G, Braun T, Feldmesser E, Efroni S, et al. Autotaxin-lysophosphatidic acid axis acts downstream of apoprotein B lipoproteins in endothelial cells. *Arterioscler Thromb Vasc Biol*. 2016;36:2058–2067. doi: 10.1161/ATVBAHA.116.308119
25. Bouchareb R, Mahmut A, Nsaibia MJ, Boulanger MC, Dahou A, Lépine JL, Laflamme MH, Hadji F, Couture C, Trahan S, et al. Autotaxin derived from lipoprotein(a) and valve interstitial cells promotes inflammation and mineralization of the aortic valve. *Circulation*. 2015;132:677–690. doi: 10.1161/CIRCULATIONAHA.115.016757
26. Kraemer MP, Mao G, Hammill C, Yan B, Li Y, Onono F, Smyth SS, Morris AJ. Effects of diet and hyperlipidemia on levels and distribution of circulating lysophosphatidic acid. *J Lipid Res*. 2019;60:1818–1828. doi: 10.1194/jlr.M093096
27. Fotopoulou S, Oikonomou N, Grigorieva E, Nikitopoulou I, Paparountas T, Thanassopoulou A, Zhao Z, Xu Y, Kontoyiannis DL, Remboutsika E, et al. ATX expression and LPA signalling are vital for the development of the nervous system. *Dev Biol*. 2010;339:451–464. doi: 10.1016/j.ydbio.2010.01.007
28. Esterbauer H, Gebicki J, Puhl H, Jürgens G. The role of lipid peroxidation and antioxidants in oxidative modification of LDL. *Free Radic Biol Med*. 1992;13:341–390. doi: 10.1016/0891-5849(92)90181-f
29. Steinbrecher UP, Parthasarathy S, Leake DS, Witztum JL, Steinberg D. Modification of low density lipoprotein by endothelial cells involves lipid peroxidation and degradation of low density lipoprotein phospholipids. *Proc Natl Acad Sci USA*. 1984;81:3883–3887. doi: 10.1073/pnas.81.12.3883
30. Cao J, Goossens P, Martin-Lorenzo M, Dewez F, Claes BSR, Biessen EAL, Heeren RMA, Balluff B. Atheroma-specific lipids in ldlr-/- and apoe-/- mice using 2D and 3D matrix-assisted laser desorption/ionization mass spectrometry imaging. *J Am Soc Mass Spectrom*. 2020;31:1825–1832. doi: 10.1021/jasms.0c00070
31. Rother E, Brandl R, Baker DL, Goyal P, Gebhard H, Tigyi G, Siess W. Subtype-selective antagonists of lysophosphatidic acid receptors inhibit platelet activation triggered by the lipid core of atherosclerotic plaques. *Circulation*. 2003;108:741–747. doi: 10.1161/01.CIR.0000083715.37658.C4
32. Navab M, Chattopadhyay A, Hough G, Meriwether D, Fogelman SI, Wagner AC, Grijalva V, Su F, Anantharamaiah GM, Hwang LH, et al. Source and role of intestinally derived lysophosphatidic acid in dyslipidemia and atherosclerosis. *J Lipid Res*. 2015;56:871–887. doi: 10.1194/jlr.M056614
33. Fulkerson Z, Wu T, Sunkara M, Kooi CV, Morris AJ, Smyth SS. Binding of autotaxin to integrins localizes lysophosphatidic acid production to platelets and mammalian cells. *J Biol Chem*. 2011;286:34654–34663. doi: 10.1074/jbc.M111.276725
34. Leblanc R, Sahay D, Houssin A, Machuca-Gayet I, Peyruchaud O. Autotaxin-β interaction with the cell surface via syndecan-4 impacts on cancer cell proliferation and metastasis. *Oncotarget*. 2018;9:33170–33185. doi: 10.18632/oncotarget.26039
35. Hosogaya S, Yatomi Y, Nakamura K, Ohkawa R, Okubo S, Yokota H, Ohta M, Yamazaki H, Koike T, Ozaki Y. Measurement of plasma lysophosphatidic acid concentration in healthy subjects: strong correlation with lysophospholipase D activity. *Ann Clin Biochem*. 2008;45(pt 4):364–368. doi: 10.1258/acb.2008.007242
36. van Meeteren LA, Ruurs P, Christodoulou E, Goding JW, Takakusa H, Kikuchi K, Perrakis A, Nagano T, Moolenaar WH. Inhibition of autotaxin by lysophosphatidic acid and sphingosine 1-phosphate. *J Biol Chem*. 2005;280:21155–21161. doi: 10.1074/jbc.M413183200
37. Meckelmann SW, Hawksworth JI, White D, Andrews R, Rodrigues P, O'Connor A, Alvarez-Jarreta J, Tyrrell VJ, Hinz C, Zhou Y, et al. Metabolic dysregulation of the lysophospholipid/autotaxin axis in the chromosome 9p21 gene SNP rs10757274. *Circ Genom Precis Med*. 2020;13:e002806. doi: 10.1161/CIRCGEN.119.002806
38. Caligiuri G, Nicoletti A, Zhou X, Törnberg I, Hansson GK. Effects of sex and age on atherosclerosis and autoimmunity in apoE-deficient mice. *Atherosclerosis*. 1999;145:301–308. doi: 10.1016/s0021-9150(99)00081-7
39. Navab M, Hough G, Buga GM, Su F, Wagner AC, Meriwether D, Chattopadhyay A, Gao F, Grijalva V, Danciger JS, et al. Transgenic 6F tomatoes act on the small intestine to prevent systemic inflammation and dyslipidemia caused by Western diet and intestinally derived lysophosphatidic acid. *J Lipid Res*. 2013;54:3403–3418. doi: 10.1194/jlr.M042051
40. Baker DL, Desiderio DM, Miller DD, Tolley B, Tigyi GJ. Direct quantitative analysis of lysophosphatidic acid molecular species by stable isotope dilution electrospray ionization liquid chromatography-mass spectrometry. *Anal Biochem*. 2001;292:287–295. doi: 10.1006/abio.2001.5063
41. Soler-Argilaga C, Danon A, Wilcox HG, Heimberg M. Effects of sex on formation and properties of plasma very low density lipoprotein in vivo. *Lipids*. 1976;11:517–525. doi: 10.1007/BF02532896
42. Beyene HB, Olshansky G, T Smith AA, Giles C, Huynh K, Cinel M, Mellett NA, Cadby G, Hung J, Hui J, et al. High-coverage plasma lipidomics reveals novel sex-specific lipidomic fingerprints of age and BMI: evidence from two large population cohort studies. *PLoS Biol*. 2020;18:e3000870. doi: 10.1371/journal.pbio.3000870
43. Wang J, Perrard XD, Perrard JL, Mukherjee A, Rosales C, Chen Y, Smith CW, Pownall HJ, Ballantyne CM, Wu H. ApoE and the role of very low density lipoproteins in adipose tissue inflammation. *Atherosclerosis*. 2012;223:342–349. doi: 10.1016/j.atherosclerosis.2012.06.003
44. Karagiannides I, Abdou R, Tzortzopoulou A, Voshol PJ, Kypreos KE. Apolipoprotein E predisposes to obesity and related metabolic dysfunctions in mice. *FEBS J*. 2008;275:4796–4809. doi: 10.1111/j.1742-4658.2008.06619.x
45. Schreyer SA, Lystig TC, Vick CM, LeBoeuf RC. Mice deficient in apolipoprotein E but not LDL receptors are resistant to accelerated atherosclerosis associated with obesity. *Atherosclerosis*. 2003;171:49–55. doi: 10.1016/j.atherosclerosis.2003.07.010
46. Huang ZH, Reardon CA, Mazzone T. Endogenous ApoE expression modulates adipocyte triglyceride content and turnover. *Diabetes*. 2006;55:3394–3402. doi: 10.2337/db06-0354
47. D'Souza K, Paramel GV, Kienesberger PC. Lysophosphatidic acid signaling in obesity and insulin resistance. *Nutrients*. 2018;10:399. doi: 10.3390/nu10040399
48. Abumrad NA, Cabodevilla AG, Samovski D, Pietka T, Basu D, Goldberg IJ. Endothelial cell receptors in tissue lipid uptake and metabolism. *Circ Res*. 2021;128:433–450. doi: 10.1161/CIRCRESAHA.120.318003
49. Mao H, Lockyer P, Li L, Ballantyne CM, Patterson C, Xie L, Pi X. Endothelial LRP1 regulates metabolic responses by acting as a co-activator of PPARγ. *Nat Commun*. 2017;8:14960. doi: 10.1038/ncomms14960
50. Ninou I, Sevastou I, Magkrioti C, Kaffe E, Stamatakis G, Thivaios S, Panayotou G, Aoki J, Kollias G, Aidinis V. Genetic deletion of Autotaxin from CD11b+ cells decreases the severity of experimental autoimmune encephalomyelitis. *PLoS One*. 2020;15:e0226050. doi: 10.1371/journal.pone.0226050
51. Triebl A, Trotzmuller M, Eberl A, Hanel P, Hartler J, Kofeler HC. Quantitation of phosphatidic acid and lysophosphatidic acid molecular species using hydrophilic interaction liquid chromatography coupled to electrospray ionization high resolution mass spectrometry. *J Chromatogr A*. 2014;1347:104–110. doi: 10.1016/j.chroma.2014.04.070